Fabrication and Characterization of Chitosan/PVA with Hydroxyapatite Biocomposite Nanoscaffolds

Dongzhi Yang,[1] Yu Jin,[1] Guiping Ma,[1] Xiangmei Chen,[2] Fengmin Lu,[2] Jun Nie[1]

[1]*State Key Laboratory of Chemical Resource Engineering, Key Laboratory of Beijing City on Preparation and Processing of Novel Polymer Materials, College of Material Science and Engineering, Beijing University of Chemical Technology, Beijing 100029, China*
[2]*Department of the Microbiology, Peking University of Health Science Center, Beijing 100083, China*

Received 21 February 2008; accepted 9 June 2008
DOI 10.1002/app.28829
Published online 10 September 2008 in Wiley InterScience (www.interscience.wiley.com).

ABSTRACT: Nanofibrous biocomposite scaffolds of chitosan (CS), PVA, and hydroxyapatite (HA) were prepared by electrospinning. The scaffolds were characterized by FTIR, SEM, TEM, and XRD techniques. Tensile testing was used for the characterization of mechanical properties. Mouse fibroblasts (L929) attachment and proliferation on the nanofibrous scaffold were investigated by MTT assay and SEM observation. FTIR, TEM, and XRD results showed the presence of nanoHA in the scaffolds. The scaffolds have porous nanofibrous morphology with random fibers in the range of 100–700 nm diameters. The CS/PVA (90/10) fibrous matrix (without HA) showed a tensile strength of 3.1 ± 0.2 MPa and a tensile modulus 10 ± 1 MPa with a strain at failure of 21.1 ± 0.6%. Increase the content of HA up to 2% increased the ultimate tensile strength and tensile modulus, but further increase HA up to 5–10% caused the decrease of tensile strength and tensile modulus. The attachment and growth of mouse fibroblast was on the surface of nanofibrous structure, and cells' morphology characteristics and viability were unaffected. A combination of nanofibrous CS/PVA and HA that mimics the nanoscale features of the extra cellular matrix could be promising for application as scaffolds for tissue regeneration, especially in low or nonload bearing areas. © 2008 Wiley Periodicals, Inc. J Appl Polym Sci 110: 3328–3335, 2008

Key words: electrospinning; chitosan; hydroxyapatite; biocomposite; nano-scaffold

INTRODUCTION

Scaffolds for tissue engineering should mimic in part the structure and biological function of the extracellular matrix (ECM). The scaffolds should provide mechanical support, deliver inductive molecules, or cells to the repair site and provide help to control the structure and function of newly formed tissue.[1–4]

An ideal 3D tissue scaffold should have similarity to natural counterparts in terms of chemical composition and physical nanofibrous structure. The structures generated by electrospinning contain nanoscale fibers with microscale-interconnected pores, resembling the topographic features of the ECM. Recently, the electrospinning approach is a rapidly growing technique in tissue engineering fields.[5–9] A broad range of materials, from natural polymers to synthetic polymers, and its composites have been processed into porous scaffolds in biomaterials and tissue engineering application.[10]

Correspondence to: J. Nie (niejun@mail.buct.edu.cn).
Contract grant sponsor: Natural Science Foundation of Beijing University of Chemical Technology.

Bone is an organic–inorganic hybrid nanobiocomposite of nanofibrous collagen and nanohydroxyapatite. On the ultrastructural level of bone, an intimate association exists between nanofibrous collagen and nanoHA crystals (4 × 50 × 50 nm).[11,12] Webster TJ reported that nanosized of HA, when compared with microsized HA, can promote cell adhesion, differentiation, proliferation, osteointegration, and deposition of calcium mineral of the surface which in turn leads to enhanced formation of new bone tissue within a short duration.[13]

Collagen and chitosan are two nature polymers that are most commonly used in tissue engineering.[14] Collagen has been used to fabricate nanofibers with diameters in the range of 100 nm to a few microns.[15] Although collagen has been extensively studied in tissue engineering, its widespread application has been hindered by poor immunogenicity, poor mechanical properties, overquick degradation rate, and higher post. Chitosan is now well-known for its numerous and interesting biological properties as a biocompatible, bioresorbable, and bioactive polymer. The chitosan scaffold for the bone tissue engineering has been widely investigated[16–18] and shown to enhance bone formation both *in vitro*[17] and *in vivo*.[19] In addition, chitosan has excellent filmogenic properties, its biodegradation kinetics is slower

than that showed by other biocompatible polymers (i.e., collagen),[20] it also has great chelating and adsorption ability of different chemicals and biological compounds, mainly due to its cationic nature. All of these properties make this biomaterial a very attractive carrier for bioactive molecules for some applications in tissue engineering. However, the major imperfection of chitosan is due to the poor workability and high brittleness, and the selection of some helpful additive with good compatibility and mechanical properties are necessary. PVA has better fiberforming, highly hydrophilic properties, and mechanical properties, simultaneously, PVA is a nontoxic, water-soluble, biocompatible, and biodegradable polymer, which is widely used in biomedical field. As biomedical materials, PVA/CS blended membrane was used to the cell culture.[21] It is reasonable to expect that the CS/PVA nanofirous membrane will play a more important role in the biomedical field. In our precious work, a series of PVA/CS nanofibrous membranes were successfully fabricated by electrospinning method.[22,23]

The aim of this work was to produce a kind of bioceramic-biopolymer nanocomposite and ultimately to apply this composite to the electrospinning of a fibrous structure. Herein, HA and CS were chosen as representative ceramic and main polymeric components, respectively, because this composite in a bulk form has already been shown to possess potential in the hard tissue surgery. As the components of the nanocomposites, CS and nanoHA are bioactive and osteoconductive.

The present article reports the electrostatic cospinning of CS/PVA and nanosize hydroxyapatite (nanoHA) as potential nanofibrous osteoconductive and bioactive nanocomposite scaffolds.

EXPERIMENTAL

Solution and electrospinning

HA nanoparticles (State pharmaceutical group Shanghai chemical reagents) were dispersed in 88 wt % acetic acid solution to form a suspension to minimize aggregation.[24] And then CS (Mw 200 KD, 85% of deacetylation, Zhejiang Golden-Shell Biochemical, Taizhou, China) and PVA (1700 of polymerization degree, 88% hydrolyzed, Kuraray, Tokyo, Japan) were added to the suspension to obtain a 7.3 wt % polymer concentration aqueous solution in a CS/PVA mass ratio of 90/10 (pH about 4.0), and the suspension was homogenized by using ultrasonic vibrator. The CS/PVA/HA dispersion was electrospun at a voltage of 25 kV (Beijing High-Voltage Research Center, Beijing, China) to create nanofibers with an needle having an inner diameter of 0.47 mm and a feeding rate of solution of 5 mL/h using a syringe pump (WZ 50C 66T, Hangzhou Jinlin Medical Appliances, Hangzhou, China). A grounded aluminum collector plate was placed 13 cm from the tip of the needle, so that the electric field magnitude was 2.5 kV/cm.

The shear viscosities of the electrospun solutions were measured at a shear rate of 344 s^{-1} with a rotational viscometer (NDJ-79, Shanghai Jichang Geology Instrument, Shanghai, China), the conductivities of the blend solutions were measured with an electric conductivity meter (DDB-6200, Shanghai Rex Xinjing Instrument, Shanghai, China).

For the propose of cell culture on the fibrous scaffold, the electrospun CS/PVA/nanoHA scaffolds were further crosslinked using 50% vapor phase glutaraldehyde in a chamber for 2 h.[25] The crosslinked membranes were then washed several times with distilled water to remove the unreacted glutaraldehyde. The crosslinked membranes were then dried overnight under vacuum.

Structural and morphological characterization

Electrospun fibers were sputter coated with gold, to observe SEM image under SEM (Hitachi *S*-4700, Hitachi, Tokyo, Japan) at an accelerating voltage of 10 kV. The average diameter of nanofibers was determined by the measurement of 30 single nanofibers with the SEM using image analysis software (Image Tool). The average pore size was taken as an average of the vertical and the horizontal dimensions of the pores. The porosity (ε) of the as spun fibrous scaffolds was estimated based on the difference between the density of CS/PVA90/10 (ρ_1) and the density of the electrospinning mats ($\rho_{2,}$), according to Eq. (1):[26]

$$\varepsilon(\%) = (1 - \rho_2/\rho_1) \times 100 \quad (1)$$

The composite electrospinning fibers for the TEM (Hitachi H-800, Hitachi, Tokyo, Japan) observation were prepared by directly depositing the as-spun fibers onto copper grids. FTIR spectra were obtained by a FTIR Spectrometer (Nicolet 5700, Thermo Electron Corp., Boston) using KBr pellets. XRD measurements were performed on an X-ray diffractometer (D/max-RB, Rigaku, Tokyo, Japan) using Cu KR radiation ($\lambda = 1.5406$E) at a current of 30 mA and an accelerating voltage of 40 kV. The spectra were recorded from $2\theta = 5$–50° at a scanning speed of 2°/min.

Mechanical characterization

Mechanical properties of electrospun membranes were determined as reported in literature[25] with a uniaxial testing machine (INSTRON1185, Instron,

Cambridge) with the use of a 10 N load cell under a cross-head speed of 10 mm/min at 23°C. All samples were cut into dog bone shape with straight flange dimensions of 20 mm × 5 mm by a standard metal mold, and then the aluminum foil was carefully peeled off. The thicknesses of the samples were measured with a digital micrometer having a precision of 1 μm. At least five samples were tested for each type of electrospun mats.

Characterization and *in vitro* biocompatibility

MTT assay

Mouse fibroblasts (L929) were cultured in RPMI1640 medium supplemented with 10% fetal bovine serum, together with 1.0% penicillin–streptomycin and 1.2% glutamine. Culture was maintained at 37°C in a wet atmosphere containing 5% CO_2. When the cells reached 80% confluence, they were trypsinized with 0.25% trypsin containing 1 m*M* EDTA.

The viabilities of cells were determined by the MTT (3-[4,-dimethylthiazol-2-yl]-2,5-diphenyltetrazolium bromide; Thiazolyl blue) assay. MTT reagent is a yellow substance which produces a dark blue formazan product when incubated with viable cells. Therefore, the level of the reduction of MTT into formazan can reflect the level of cell metabolism. For the MTT assay, the prepared crosslinked membranes with 1.5 cm in diameter were sterilized with highly compressed steam for 15 min and placed in wells of 24-well culture plate, respectively. The samples were then incubated in 1 mL RPMI1640 medium at 37°C for 24 h. At the end of this period, the membranes were removed, and the so-called extracts were obtained. L929 cells were seeded in wells of 96-well plate at a density of 10^3 cells per well. After incubated for another 24 h, the culture medium was removed and replaced with the as-prepared extraction medium and incubated for another 24 h, and then 100 μL MTT solution was added to each well. After 3 h incubation at 37°C, 200 μL of dimethyl sulfoxide was added to dissolve the formazan crystals. The dissolved solution was swirled homogeneously about 10 min by the shaker. The optical density of the formazan solution was detected by an ELISA reader (Multiscan MK3, Labsystem, Finland) at 570 nm.

For the reference purpose, cells were seeded to a fresh culture medium (negative control) with same seeding condition, respectively. Each assay was performed five times in triplicate.

SEM observation of cell culture and adhesion

The sterilized CS/PVA/HA (or without HA) scaffolds were extensively washed three times with sterile phosphate buffered saline (PBS) and transferred to individual 24-well tissue culture plates. Aliquots (1 mL) of mouse fibroblasts (L929) suspension with 1.5×10^4 cell/mL were seeded on the sample membranes. After 48 h of culture, cellular constructs were harvested, rinsed twice with PBS to remove nonadherent cells, and subsequently fixed with 3.0% glutaraldehyde at 4°C for 4 h. After that the samples were dehydrated through a series of graded ethanol solutions and air dried overnight. Dry samples were sputtered with gold for observation of cell morphology on the surface of the scaffolds by SEM.

RESULTS AND DISCUSSION

CS/PVA was coelectrospun with nanoHA to obtain bioactive nanocomposite scaffolds with filler content from 0 to 10 wt %. Higher percentage loading of HA resulted in an agglomeration of nanosized HA particles.

The structure and morphology of nanocomposite fibers were shown in Figure 1(a–e). The viscosity, conductivity for all of the as-prepared spinning dopes were summarized in Table I.The electrospun nanocomposite fibers formed a nonwoven fabric structure having diameters in the range of 100–700 nm. Figure 2 indicates the frequency distribution of the diameters of electrospun fibers with different HA content. In natural bone tissues, the organic matrix fibers have diameters in the range from 100 to 450 nm.[22] The present CS/PVA-nanoHA composite scaffolds have a majority of the fibers in the upper range. The majority of the electrospun CS/PVA fibers have diameter in the range from 100 to 400 nm. When the loading of nanoHA increased to 5%, the distribution maximum shifts to higher diameter region. This indicated that the diameter of composite fibers increases with increase of HA content. With higher nanoHA content (10 wt %), the effect of concentration (viscosity) on fiber diameter plays an important role and results in a broader diameter distribution and poor spin-ability (Fig. 1 day). The vapor phase crosslinking of CS/PVA using glutaraldehyde has effect on the morphology of fibers [Fig. 1(e)]. The crosslinked CS/PVA scaffolds exhibited a higher dimensional stability in aqueous medium due to chemical crosslinking.

Nanosize HA particles tend to form aggregates when suspended in aqueous solutions. Aisha Bishop reported that high concentration of acetic acid was introduced to the prespinning solution could improve the dispersion of HA throughout the polymeric matrix.[24] To stabilize the nanoparticles, the HA nanoparticles were dispersed in 88 wt % acetic acid solution to form a suspension to minimize aggregation.

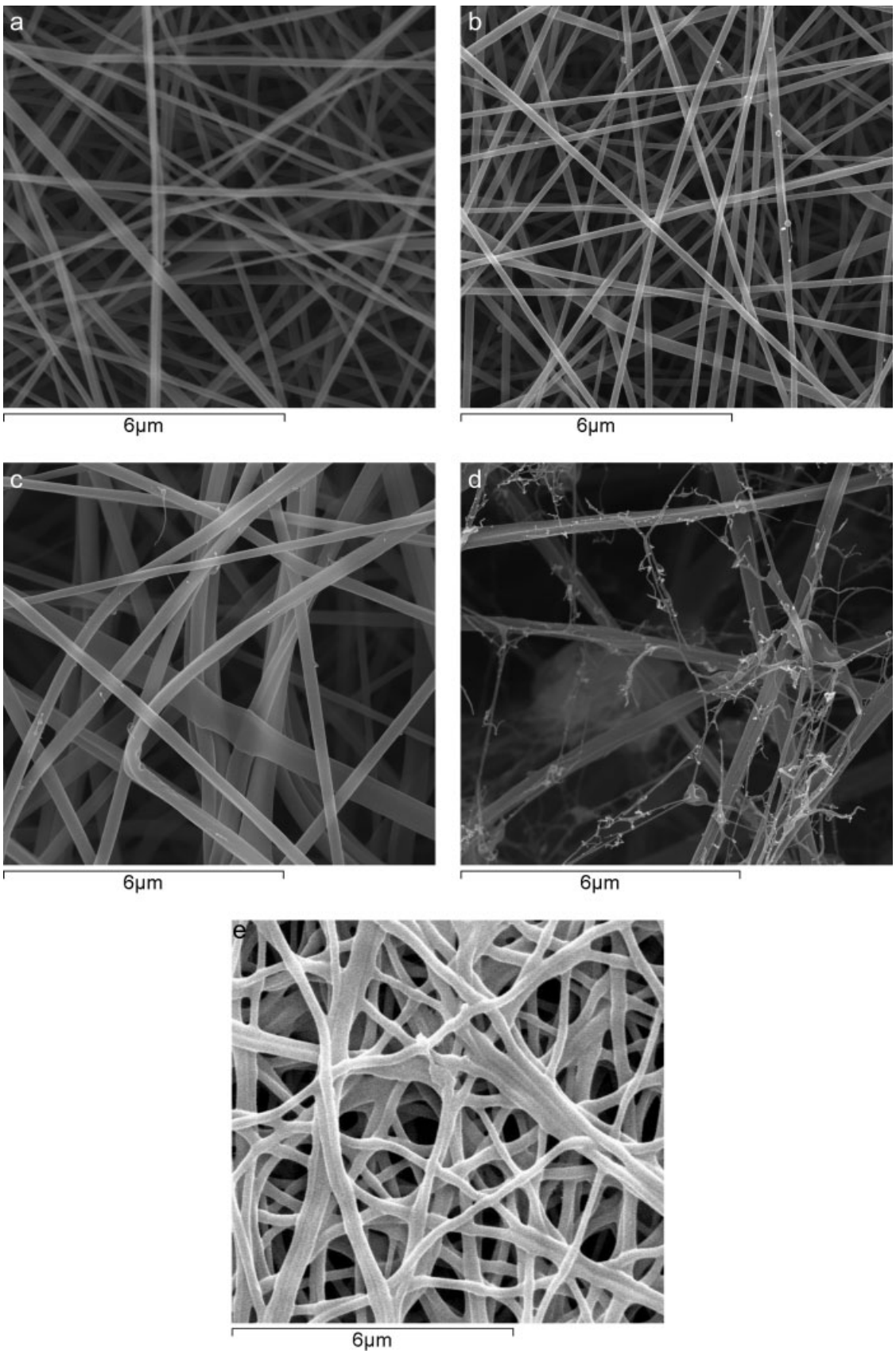

Figure 1 SEM photographs of electrospun scaffolds. (a) CS/PVA fibers, (b) CS/PVA + 2% HA (uncrosslinked), (c) CS/PVA + 5% HA (uncrosslinked), (d) CS/PVA + 10% HA (uncrosslinked), and (e) CS/PVA + 5% HA (crosslinked).

TABLE I
Properties of As-Prepared Spinning Solutions and Nanofibers (Noncross-linked)

HA (wt %)	Viscosity (cp) (25°C)	Conductivity (ms/cm)	Average diameter (nm)	Elastic modulus (MPa)	Ultimate strength (MPa)	Strain at failure (%)	Average pore size (μm)	Porosity (%)
0	477	1.20	209	12 ± 1	3.1 ± 0.2	21.1 ± 0.6	2.5 ± 0.6	85.1 ± 5.3
2	760	1.21	205	100 ± 8	3.6 ± 0.4	10.9 ± 0.4	2.3 ± 0.4	86.7 ± 8.9
5	1300	1.22	349	65 ± 4	3.2 ± 0.3	13.8 ± 0.7	4.0 ± 1.5	80.2 ± 10.3
10	1890	1.27	–	47 ± 4	2.5 ± 0.4	10.5 ± 0.6	–	–

The effect of HA content (viscosity) of electrospun solution resulted in a broader diameter distribution and poor spinability.

Figure 3 showed TEM images of HA nanoparticles and CS/PVA/HA nanofibers. The needle-like HA particles were about (30–60 nm) × (10–15 nm), which was very similar to the apatite in living bone. In some regions of the fibers, the nanoparticles were well dispersed in the fiber [Fig. 3(b)]. In some cases, that is, the content of HA in composite was up to 10%, and the nanoparticles tended to aggregate.

The existence of HA in the electrospun fiber scaffold was further confirmed by FTIR and XRD. The FTIR spectra (Fig. 4) of the electrospun CS/PVA/HA composite fibers showed characteristic peaks for CS/PVA and HA. The absorption bands at 1655 and 1548 cm^{-1} (amide I and amide II from CS) and bands at 3450 cm^{-1}(νOH), 2950 cm^{-1}(νCH_2), 1740 cm^{-1}(νC=O of PVA), 1100 cm^{-1}(νC—O), and 852 cm^{-1}(ν C—C) were observed in CS/PVA and CS/PVA/HA composite fibers [Fig. 4(a,b)]. The HA characteristic peak of νPO_4^{3-} stretching band around 1050 cm^{-1} was found in spectrum Figure 4(b,c).

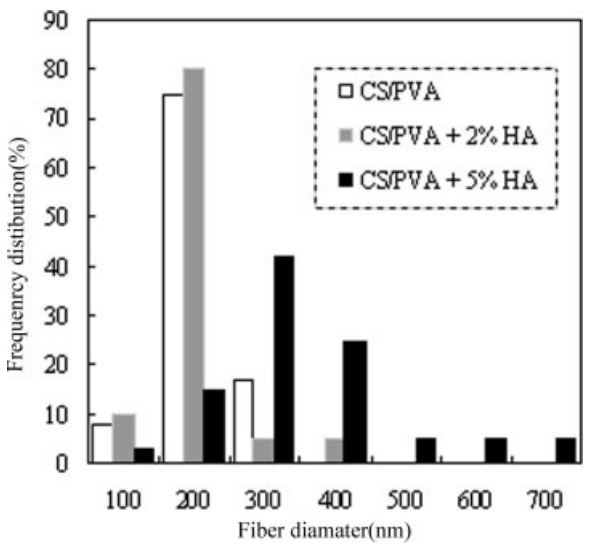

Figure 2 Frequency distribution of fiber diameters of scaffold. As the HA content increases, the distribution maximum shifts to higher diameter region.

X-ray diffraction spectra showed that CS/PVA blend nanofibers membrane showed a relative obtuse and broad peak around $2\theta = 20.1^\circ$ [Fig. 5(a)]. For that of the composite [Fig. 5(b,c)], most of characteristic peaks of HA were distinctly observed, that is, the reflections 002, 211, 300, 130, 222, and 213 centered at 25.8, 32.1, 34.0, 39.9, 46.6, and 49.5° 2θ values corresponding to the HA crystals.

The mechanical properties of the nanocomposite fibers were evaluated by a tensile test. The stress–strain curve of the samples was shown in Figure 6. When compared with pure CS/PVA, as the HA content increased to 10%, the ultimate strength increased to 3.6 ± 0.4 MPa and the tensile modulus 100 ± 8 MPa with a strain at failure 10.9 ± 0.4%. The increase in tensile strength may be attributed to an increase in rigidity, because HA is typical of hard inorganic phases. Further increase in HA content decreased the tensile properties of nanocomposite fibers. Higher percentage loading of HA might have resulted in integrating of the nanoHA powder in the CS/PVA matrix, because failure of the composite materials usually occurs at the interface of the polymer and the HA. Furthermore, the intermediate between HA particles was a very weak interface.

The ultimate tensile strength of uniaxially tested natural articular cartilage tissues ranges from 9 to 18 MPa, with an ultimate strain of 15–120%.[27] Mechanical property measurements showed that the electrospun CS/PVA/HA scaffolds were not able to attain high tensile strength, but it may be a potential candidate application in tissue engineering of low and/or nonload bearing areas. It has also been reported that chondrocyte adhesion and proliferation on polymer/nanoHA composite materials are better than for the pure polymer.[28]

To examine the interaction of the nanofibrous scaffold with tissue cells, an indirect cytotoxicity test was conducted by using mouse fibroblasts (L929) cells. Even though we were interested in using the obtained composite mats as potential bone scaffolds, it was mandatory to test the materials with L929 just to comply with the ISO10993-5 standard test

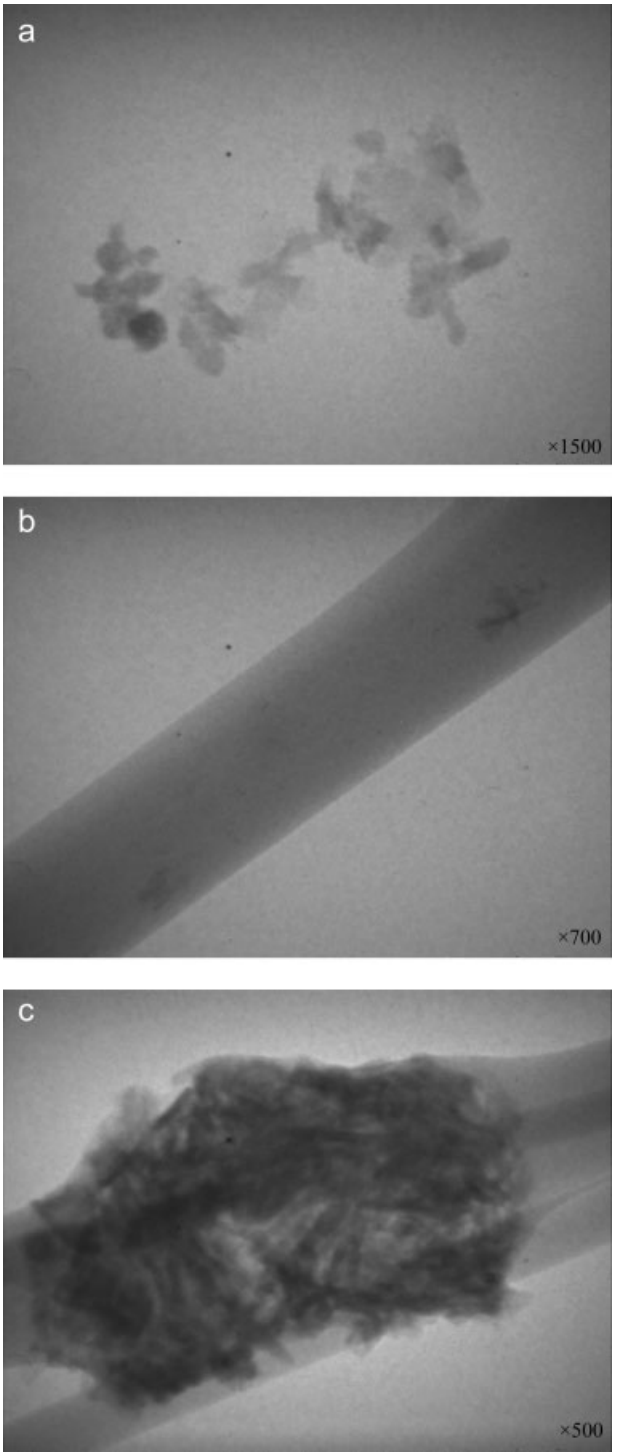

Figure 3 TEM observation of HA nanoparticles and CS/PVA/HA fibers. (a) HA nanoparticles, (b) CS/PVA + 2%HA, and (c) CS/PVA + 10%HA.

method. Figure 7 showed the absorbance obtained from an MTT assay of the mouse fibroblasts (L929) which were cultured with the extraction media of the scaffolds in comparison with control. For L929, the absorbance intensity of all the fibrous scaffolds was similar level to that of control during 24 h.

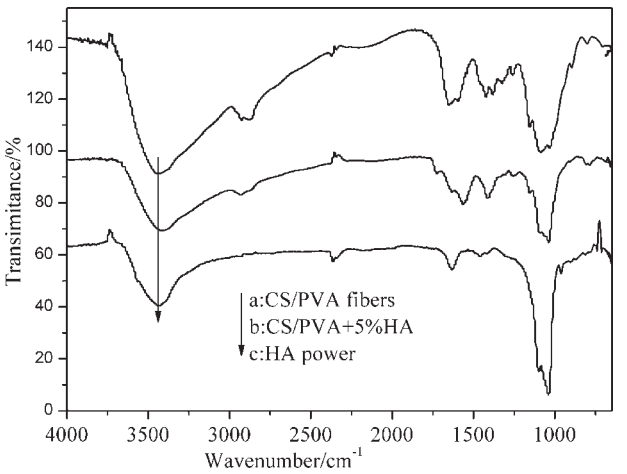

Figure 4 FTIR spectra of HA powder, CS/PVA and CS/PVA + 5% HA composite scaffolds. The increased peak around 1050 cm^{-1} in composite spectra are due to the HA.

Although absorbance intensity CS/PVA + 10% HA was lower than the other two samples, but its absorbance ratios maintained at least 80% cultured (Absorbance of sample/Absorbance of control). All of the obtained results clearly suggested that electrospun CS/PVA and CS/PVA/HA fibers were nontoxic to mouse fibroblasts and posed as good candidates to be used as tissue scaffolds.

As shown in Figure 8, the SEM of the cells cultured on the CS/PVA/HA nanocomposite fiber for 2 days shows that the cells spread actively on the fibrous mesh in intimate contact, and cells were attached to the surfaces by discrete filopodia and exhibited numerous microvillus on their surfaces. Cells adhered well. These results suggested good

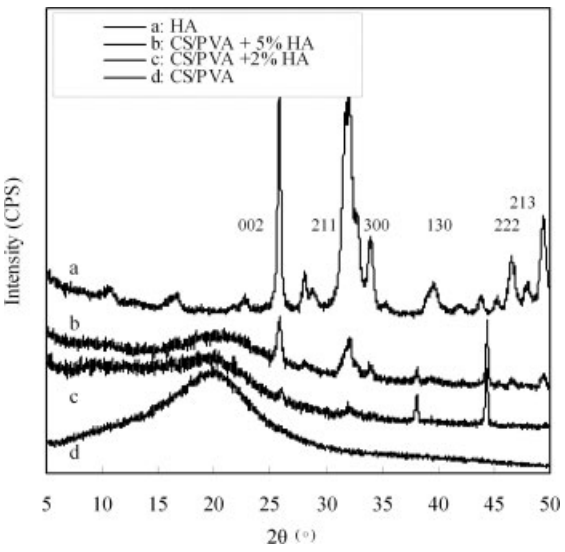

Figure 5 XRD patterns of HA powder, CS/PVA and CS/PVA/HA composite fibers.

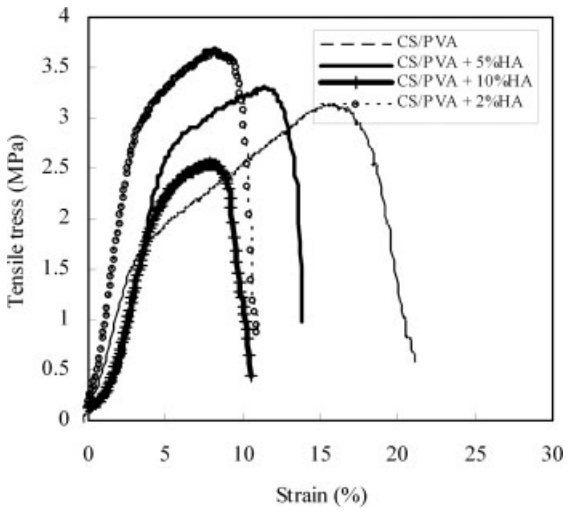

Figure 6 Tensile curves of CS/PVA and CS/PVA/HA composite fibrous scaffold.

cell viability on the CS/PVA/HA nanocomposite fibers.

CONCLUSIONS

Biocomposite nano-scaffolds of CS/PVA/HA were prepared by electrospinning. SEM analyses showed a well interconnected pore network structure with nanofibrous morphology of randomly oriented fibers in the diameter range 100–700 nm. The fiber diameter increased with an increase in nanoHA content. The pure CS/PVA fibrous matrix (without nanoHA) showed an average tensile strength of 3.1 ± 0.2 MPa and tensile modulus 10 ± 1 MPa with a strain in failure of 21.1 ± 0.6%. Increase of HA content up to 5%, increased ultimate strength and tensile modulus and decreased strain in failure, but further increased HA content, decreased the ultimate strength and strain in failure. Cell culture SEM imaging showed that the mouse fibroblast might grow on the surface of nanofibrous structure, and the cell morphology and viability were maintained. In conclusion, based on our observations, the CS/PVA/HA biological nanocomposite fiber was considered as a promising material for bone tissue regeneration.

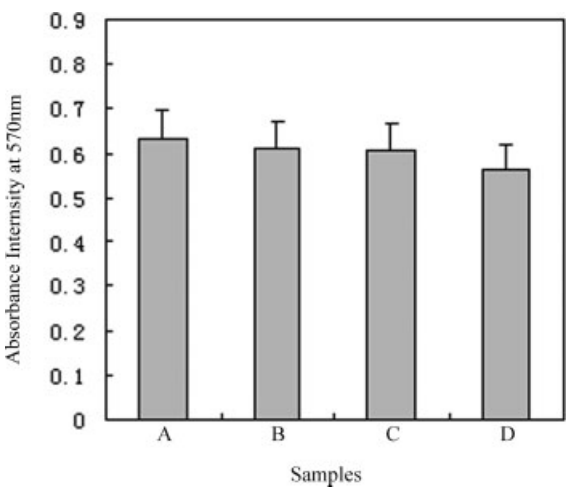

Figure 7 Formazan absorption (A570 nm) in MTT assays mouse fibroblasts (L929) seeded on the samples for 24 h. A: control, B: crosslinked CS/PVA membrane, C: crosslinked CS/PVA/HA(5%) membrane, D: crosslinked CS/PVA/HA(10%) membrane.

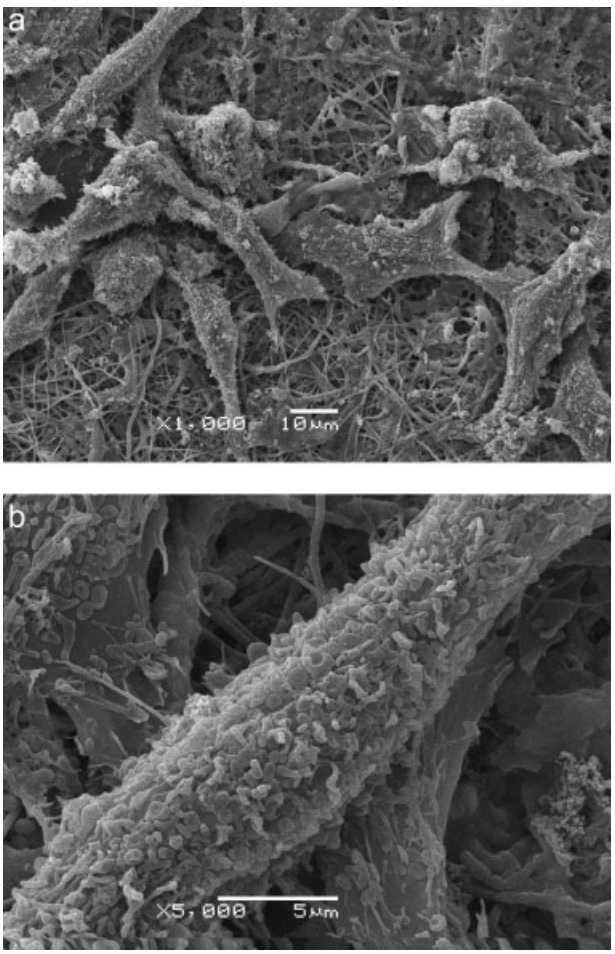

Figure 8 SEM images of mouse fibroblasts seeded on fibrous membranes of HA-CS/PVA after 2 day culture (a) 1000× magnification, (b) 5000× magnification.

Program for Changjiang Scholars and Innovative Research Team in University is appreciated.

References

1. Boland, E. D.; Wnek, G. E.; Simpson, G. D.; Pawlowski, K. J.; Bowlin, G. L. J Macromol Sci Pure Appl Chem 2001, A38, 1231.
2. Li, W. J.; Laurencin, C. T.; Caterson, E. J.; Tuan, R. S.; Ko, F. K. J Biomed Mater Res 2002, 60, 613.
3. Stitzel, J. D.; Pawlowski, K.; Wnek, G. E.; Simpson, D. G.; Bowlin, G. L. J Biomater Appl 2001, 16, 22.
4. Hirano, Y.; Mooney, D. J. Adv Mater 2004, 16, 17.
5. Dzenis, U. Science 2004, 304, 1917.

6. Li, D.; Xia, Y. Adv Mater 2004, 16, 1151.
7. Kim, H. W.; Song, J. H.; Kim, H. E. Adv Funct Mater 2005, 15, 1988.
8. Yoshimoto, H.; Shin, Y. M.; Terai, H.; Vacanti, J. P. Biomaterials 2003, 24, 2077.
9. You, Y.; Min, B. M.; Lee, S. J.; Lee, T. S.; Park, W. H. J Appl Polym Sci 2005, 95, 193.
10. Huang, Z. M.; Zhang, Y. Z.; Ramakrishna, M. K. S. Compos Sci Technol 2003, 63, 2223.
11. Rho, J. Y.; Kuhn-Spearing, L.; Zioupos, P. Med Eng Phys 1998, 20, 92.
12. McConnell, D. Clin Orthop Relat Res 1962, 23, 253.
13. Webster, T. J.; Siegel, R. W.; Bizios, R. Biomaterials 2000, 21, 1803.
14. Majeti, N. V. React Funct Polym 2000, 46, 1.
15. Matthews, J. A.; Wnek, G. E.; Simpson, D. G.; Bowlin, G. L. Biomacromolecules 2002, 3, 232.
16. Park, Y. J.; Lee, Y. M.; Park, S. N.; Sheen, S. Y.; Chung, C. P.; Lee, S. J. Biomaterials 2000, 21, 153.
17. Klokkevold, P. R.; Vandemark, L.; Kenney, E. B.; Bernard, G. W. J Periodontol 1996, 67, 1170.
18. Gutowska, A.; Jeong, B.; Jasionowski, M. Anatomical Record 2001, 263, 342.
19. Malette, W. G.; Quigley, H.; Adickes, E. D. Chitin in nature and technology. In: Muzzarelli, R.; Jeuiaux, C.; Gooddy, G. W., Eds. Chitosan Effect in Nature and Technology; Plenum Press: New York, 1986; p 435–442.
20. Somashekar, D.; Joseph, R. Bioresour Technol 1996, 55, 35.
21. Chuang, W. Y.; Young, T. H.; Yao, C. H.; Chi, W. Y. Biomaterials 1999, 20, 1479.
22. Zhen, H. P.; Nie, J.; Guo, S.; Sun, J. F.; Yang, D. Z. Acta polymerica sinica 2007, 6, 230.
23. Zhou, Y. S.; Yang, D. Z.; Nie, J. J Appl Polym Sci 2006, 102, 5692.
24. Bishop, A.; Balazsi, C. J.; Yang, H. C. Polym Adv Technol 2006, 17, 902.
25. Yang, D. Z.; Li, Y. N.; Nie, J. Carbohydr Polym 2007, 69, 538.
26. Wutticharoenmongkol, P.; Sanchavanakit, N.; Pavasant, P.; Supaphol, P. Macromol Biosci 2006, 6, 70.
27. Woo, S.; Buckwalter, J. In American Academy of Orthopedic Surgeons Symposium; Woo, S.; Buckwalter, J., Eds.; American Academy of Orthopaedic Surgeons: Savannah, Georgia 1988, p 401.
28. Hong, Z.; Zhang, P.; He, C.; Qiu, X.; Liu, A.; Chen, L.; Chen, X.; Jing, X. Biomaterials 2005, 26, 6296.